Original papers
Nanostructured, nanoscale materials and nanodevices

УДК 661.866.2+57.083.37 DOI: 10.17277/jamt-2026-11-01-069-080

Surface modification of Gd_2O_3-graphene by different functionalities and captopril molecules

© Evgeniya V. Suslova[a]✉, Sergey V. Yakovlev[b], Denis A. Shashurin[c, d], Daria A. Ipatova[a], Dmitry A. Skvortsov[a], Sergey V. Maximov[a], Konstantin I. Maslakov[a], Yana B. Platonova[a], Serguei V. Savilov[a, b], Georgy A. Chelkov[e]

[a] *Lomonosov Moscow State University, Bld. 3, 1, Leninskie Gory, Moscow, 119991, Russian Federation,*
[b] *Kurnakov Institute of General and Inorganic Chemistry RAS, 31, Leninskii Av., Moscow, 119991, Russian Federation,*
[c] *Medicine Research-Educational Institute, Lomonosov Moscow State University, Bld. 1, 27, Lomonosovskii Av., Moscow, 119991, Russian Federation,*
[d] *E.I. Chazov National Medical Research Center of Cardiology, 15A, Chazov St., Moscow, 121552, Russian Federation,*
[e] *Joint Institute for Nuclear Research, 6, Joliot-Curie, Dubna, 141980, Russian Federation*

✉ suslova@kge.msu.ru

Abstract. Nanoparticles of insoluble Gd^{3+} compounds are considered to be a promising direction of development of multimodal contrast agents for magnetic resonance imaging and computed tomography. The surface of such nanoparticles can be functionalized by molecules or chemical groups with high affinity to specific biopolymers. In the present work, we proposed a novel approach to obtaining such selective structures. At the first stage, Gd_2O_3 nanoparticles of 1–2 nm size stabilized on the surface of graphene nanoflakes (GNFs) were produced. Their further graphitization produced core-shell (Gd_2O_3/GNFs)@C particles. Treatment of these particles with nitric acid vapor resulted in the formation of surface carboxyl groups. Further reaction with $SOCl_2$ produced (Gd_2O_3/GNFs)@C-COCl particles, which were used to obtain the esters containing the allyl fragment (Gd_2O_3/GNFs)@C-COOAll or molecules of specific inhibitor of angiotensin-converting enzyme captopril. All products were characterized by transmission electron microscopy, thermogravimetric analysis, IR and X-ray photoelectron spectroscopy. The results of these analyses confirmed that the functionalization of the particles by carboxyl, acyl chloride or allyl groups, as well as captopril molecules, did not change their morphology or the size of Gd_2O_3 cores. The cytotoxicity of (Gd_2O_3/GNFs)@C-COOH, (Gd_2O_3/GNFs)@C-COOAll and (Gd_2O_3/GNFs)@C-captopril particles was assessed.

Keywords: gadolinium; graphene; allyl; captopril; nanoparticles; surface modification; contrast agent; cytotoxicity.

For citation: Suslova EV, Yakovlev SV, Shashurin DA, Ipatova DA, Skvortsov DA, Maximov SV, Maslakov KI, Platonova YaB, Savilov SV, Chelkov GA. Surface modification of Gd_2O_3-graphene by different functionalities and captopril molecules. *Journal of Advanced Materials and Technologies*. 2026;11(1):069-080. DOI: 10.17277/jamt-2026-11-01-069-080

Поверхностная модификация Gd_2O_3-графен различными группами и молекулами каптоприла

Е. В. Суслова[a]✉, С. В. Яковлев[b], Д. А. Шашурин[c, d], Д. А. Ипатова[a], Д. А. Скворцов[a], С. В. Максимов[a], К. И. Маслаков[a], Я. Б. Платонова[a], С. В. Савилов[a, b], Г. А. Шелков[e]

[a] *Московский государственный университет имени М. В. Ломоносова, Ленинские Горы, 1, стр. 3, Москва, 119991, Российская Федерация,*
[b] *Институт общей и неорганической химии им. Н. С. Курнакова РАН, Ленинский пр., 31, Москва, 119071, Российская Федерация,*

[c] *Медицинский научно-образовательный институт МГУ имени М. В. Ломоносова, Ломоносовский пр., 27, стр. 1, Москва, 119991, Российская Федерация;*
[d] *Национальный медицинский исследовательский центр кардиологии имени академика Е.И. Чазова, ул. Чазова, 15А, Москва, 121552,Российская Федерация,*
[e] *Международная межправительственная организация «Объединенный институт ядерных исследований», ул. Джолио-Кюри, 6, Дубна, 141980, Российская Федерация*

✉ suslova@kge.msu.ru

Аннотация. В настоящее время одним из направлений разработки новых мультимодальных контрастных агентов для методов магнитно-резонансной и компьютерной томографии является создание препаратов на основе наночастиц нерастворимых соединений Gd^{3+}. Поверхность таких наночастиц можно функционализировать якорными молекулами или группами, селективными относительно определенных биополимеров. В представленной работе предложен новый метод для создания таких селективных структур. На первом этапе процесса получены наночастицы Gd_2O_3 с размером 1…2 нм, стабилизированные на поверхности малослойных графеновых фрагментов (МГФ). Последующая графитизация поверхности частиц Gd_2O_3/МГФ позволила получить частицы со структурой типа ядро-оболочка (Gd_2O_3/МГФ)@C. Обработка частиц (Gd_2O_3/МГФ)@C парами азотной кислоты привела к формированию поверхностных карбоксильных групп. При взаимодействии (Gd_2O_3/МГФ)@C-COOH с $SOCl_2$ выделены частицы (Gd_2O_3/МГФ)@C-COCl. При замещении атомов хлора в составе ацилхлоридных групп получены сложные эфиры, содержащие аллиловые фрагменты (Gd_2O_3/МГФ)@C-COOAll или молекулы специфического ингибитора ангиотензин-превращающего фермента каптоприла. Все продукты охарактеризованы методами просвечивающей электронной микроскопией, термогравиметрического анализа, ИК- и рентгено-фотоэлектронной спектроскопией. Показано, что функционализация карбоксильными, ацилхлоридными группами, как и молекулами каптоприла и аллиловыми фрагментами не меняет морфологию частиц, а размер Gd_2O_3 остается неизменным. Представлены результаты оценки цитотоксичности частиц (Gd_2O_3/МГФ)@C-COOH, (Gd_2O_3/МГФ)@C-COOAll и (Gd_2O_3/МГФ)@C-каптоприл.

Ключевые слова: гадолиний; графен; аллил; каптоприл; наночастицы; поверхностная модификация; контрастный агент; цитотоксичность.

Для цитирования: Suslova EV, Yakovlev SV, Shashurin DA, Ipatova DA, Skvortsov DA, Maximov SV, Maslakov KI, Platonova YaB, Savilov SV, Chelkov GA. Surface modification of Gd_2O_3-graphene by different functionalities and captopril molecules. *Journal of Advanced Materials and Technologies*. 2026;11(1):069-080. DOI: 10.17277/jamt-2026-11-01-069-080

1. Introduction

Chelated Gd^{3+} complexes of polycarbonic acids are widely used in modern clinical practice as contrast agents for magnetic resonance imaging (MRI) [1]. Nanoparticles of insoluble Gd^{3+} compounds and iron oxides are an alternative to the complexes described in [2, 3]. Surface modification of nanoparticles with organic groups or molecules ensures the selectivity of the contrast agent to certain cells, proteins, biological molecules or biopolymers [4, 5]. Nanoparticles accumulate in certain areas assisting the detection of pathologies including the smallest ones. Moreover, the resolution of image increases due to higher signal-to-noise ratio of contrasting nanoparticles. Thus this ultimately leads to the targeted controlled delivery and significant reduces the administered doses. Moreover, the surface groups prevent aggregation of nanoparticles [6].

Nanoparticle contrast agents typically represent oxide particles encapsulated in mesoporous silica [7, 8], clays or lipids [9]. An example of such structure is the core-shell γ-Fe_2O_3@SiO_2@captopril system described in [10], where the core-shell nanoparticles are functionalized with captopril – inhibitor of angiotensin-converting enzyme.

Two-dimensional carbon nanomaterials, particularly graphene and its derivatives, represent a versatile matrix for nanoparticle stabilization [11]. At the same time, the graphene surface can be functionalized with different groups and molecules [12–14]. Among the core-shell particles with a metal oxide core and functionalized graphene shell, the synthesis of magnetic Fe_3O_4 nanoparticles encapsulated in C_3N_4 nanosheets was described in [15]. The surface of these particles was modified by 1,3-dibromo-propane and finally the captopril molecules. The resulting composite Fe_3O_4@C_3N_4–Pr^- captopril was assessed as an effective catalyst in the synthesis of 1,2,3,6-tetrahydropyrimidine and 2-amino-4H-chromene derivatives [15].

Previously we described the synthesis and physicochemical characteristics of 1–2 nm Gd_2O_3 particles stabilized on the graphene nanoflake (GNF) surface [16]. The graphitic core-shell (Gd_2O_3/GNFs)@C and oxidized (Gd_2O_3/GNFs)@C-COOH particles are affective contrast agents for MRI [7] and photon-counting computed tomography [17]. These particles can be further functionalized with more specific surface groups. In particular, we have proposed further conversion of carboxyl groups into acyl chloride groups and then into alloxide ester. The (Gd_2O_3/GNFs)@C-COOAll (All = allylic radical) particles were polymerized in the presence of acrylic acid and acrylamide monomers to produce contrasting hydrogels for implantable systems [18].

In the present study, we assessed the possibility of further functionalization of (Gd_2O_3/GNFs)@C nanoparticles and described six-steps synthesis and characteristics of their captopril-modified derivatives. Additionally, an assessment of the cytotoxicity of resulting particles and intermediate synthetic products (Gd_2O_3/GNFs)@C-COOH and Gd_2O_3@C-COOAll was made.

2. Experiment

2.1. Synthetic process

Graphene nanoflakes (GNFs) were synthesized by pyrolytic decomposition of hexane (99.8 %, Reachim) at 900–950 °C for 30 min in the presence of the MgO template. The prepared GNFs were purified from MgO by refluxing with HCl (99.9 %, Reachim) for 8 h and followed by rinsing with distilled water and drying at 110 °C for 4 h. Oxidation of the GNF surface was produced by refluxing with HNO_3 for 1 h.

Nanoparticles Gd_2O_3 were synthesized by impregnation of oxidized GNFs with a water-ethanol solution of $Gd(NO_3)_3{\cdot}6H_2O$ (99.9 %, China Northern Rare Earth Group High-Tech Co. Ltd.) with subsequent nitrate decomposition under N_2 atmosphere at 450 °C according to [16].

The synthesis of (Gd_2O_3/GNFs)@C, (Gd_2O_3/GNFs)@C-COOH, (Gd_2O_3/GNFs)@C-COCl and (Gd_2O_3/GNFs)@C-COOAll were previously described elsewhere [18–20]. In brief, Gd_2O_3/GNF particles were carbonized under CH_4 (99.99 % Moscow Gas Processing Plant, Moscow, Russia) flow in the fixed-bed reactor at 400–450 °C for 30 min to obtain core-shell (Gd_2O_3/GNFs)@C particles [19]. Their surface was modified by HNO_3 vapors. For this purpose (Gd_2O_3/GNFs)@C sample was placed in an open vessel in an atmosphere of boiling HNO_3 for 1 h, which led to (Gd_2O_3/GNFs)@C-COOH formations described [20].

Carboxylate groups in (Gd_2O_3/GNFs)@C-COOH were modified with $SOCl_2$ to obtain acyl chloride (Gd_2O_3/GNFs)@C-COCl [18, 21]. Reaction of the (Gd_2O_3/GNFs)@C-COCl sample with sodium alloxide NaOAll resulting in the substitution of the chloride group with the alloxide group producing (Gd_2O_3/GNFs)@C-COOAll in accordance with [18].

(Gd_2O_3/GNFs)@C covalently bonded with captopril molecules was synthesized *via* reaction of (Gd_2O_3/GNFs)@C-COCl with captopril. 1.43 g of (Gd_2O_3/GNFs)@C-COCl was dispersed in the 30 mL dry toluene under sonication for 30 min. Then 0.06 g of captopril (> 98 %, TCI, Tokyo Chem. Ind., Japan) was added to the reaction mixture under an Ar (99.993 %, Logica Ltd., Moscow, Russia) atmosphere. The mixture was refluxed for 24 h, cooled to room temperature, filtered and washed with ethanol. The (Gd_2O_3/GNFs)@C-captopril sample was dried at room temperature for 12 h.

2.2. Characterization techniques

High resolution transmission electron microscopy (HRTEM) images were recorded on a JEOL 2100F/Cs (Jeol, Japan) microscope operated at 200 kV and equipped with an UHR pole tip, a spherical aberration corrector (CEOS, Germany), and an EEL spectrometer (Gatan, Germany).

The surface groups in the synthesized particles were analyzed by IR spectroscopy using an FSM 1202 FTIR spectrometer (Infraspek, Russia). Prior to the analysis the samples were ground in an agate mortar with dried KBr (98.5 %, China) at weight ratio of 1 : 9 and pressed into tablets using hydraulic press (OMEC, Italy). A pellet of pure KBr was used for reference spectra. The measurements were carried out with the accumulation of 30 scans in the range from 400 to 4000 cm^{-1} with a resolution of 4 cm^{-1}.

Thermal stability of the materials was studied using the simultaneous thermal analyzer STA 449 F3 (NETZSCH, Germany). A portion of material in an Al_2O_3 crucible was placed in the furnace of device, which was purged with air flow of 50 $mL{\cdot}min^{-1}$ during the measurement, while the weighing block was purged with a flow of protective nitrogen (99.999 %, NII KM) gas of 20 $mL{\cdot}min^{-1}$. The sample was heated at a rate of $1°{\cdot}min^{-1}$ to 40° and kept in a waiting mode for 20 min until the scale readings

stabilized. Then heating was carried out at a rate of 10°·min^{-1} up to 1000° while simultaneously recording thermogravimetry (TG) and differential thermal analysis (DTA) signals. To determine the composition of gases emitted during the heating, TG coupled with mass spectra analysis was used in STA 449 C Jupiter combined with QMS 403C Aëolos quadrupole mass spectrometer (both NETZSCH, Germany). The furnace was purged with an air flow of 80 mL·min^{-1}, and the weighing block with an argon (99.993 %, NII KM) flow of 40 mL·min^{-1}. Ionization of gas molecules was achieved by electron impact, and ion separation was carried out by a quadrupole of mass spectrometer in the range from 10 to 100 a.u.

The content of oxygen, carbon, gadolinium, chlorine and sulfur were confirmed by X-ray photoelectron spectroscopy (XPS) using a Kratos Axis Ultra DLD instrument with the monochromatic AlKα source (1486.6 eV) (Kratos Analytical, UK). The survey XPS spectra were recorded at a pass energy of 160 eV while a pass energy of 40 eV was used for high-resolution scans.

2.3. Cytotoxicity

The cytotoxicity of synthesized (Gd_2O_3/GNFs)@C-COOH, (Gd_2O_3/GNFs)@C-COOAll and (Gd_2O_3/GNFs)@C-captopril nanoparticles was investigated by MTT test. All samples were kept in glass boxes for 4 h at 80 °C before testing to ensure sterility. The HEK293T cells (2500 cells/well) were plated out in 100 μL of DMEM/F12 media (PanEco LLC, Russia) in a 96-well plate and incubated at 37 °C, 5 % CO_2 for 18 h before treatment. The nanoparticles were suspended with cell growth media and methylcellulose (Sigma-Aldrich, USA) and then added to cells. The maximum concentration of each sample was 1600 μg [Gd^{3+}]·mL^{-1}, dilution step ×2: methylcellulose concentration was 2 % in each well. Three experimental replicates (wells) were used for each concentration of each sample. After adding the particles, the cells were incubated for 72 h, and then metabolic activity was assessed using the MTT test. Doxorubicin was used as a comparison drug. At the end of the incubation, MTT (Paneco LLC, Russia) was added into the media (up to 0.5 mg·mL^{-1}), the cells were incubated for 2 h, followed by removing the media and addition of 100 μL of DMSO. The amount of MTT reduced by cells to its blue formazan derivative was measured spectrophotometrically at 565 nm using a VICTOR microplate reader (PerkinElmer, Singapore) and normalized to the values for cells incubated without compounds. The optical density at 670 nm was additionally measured to subtract the value of turbidity caused by particles. IC_{50abs} was calculated with "GraphPad Prism 5" software (GraphPad Software, Inc., San Diego, CA).

3. Results and Discussion

We proposed a six-step process that includes the synthesis of (Gd_2O_3/GNFs)@C-COOAll as described in [18] followed by a newly proposed step to synthesize (Gd_2O_3/GNFs)@C-captopril (Fig. 1). This scheme demonstrates all intermediate products and simplifies their characterization by several methods.

The synthesis starts from GNF particles produced as described earlier [18, 22]. In brief, GNF particles replicate the shape of template particles and contain 7–10 stacked graphene layers (Fig. 2*a*, *b*). In the first step of the synthesis the GNF surface is oxidized to provide more uniform distribution of Gd^{3+} ions in the second step. The Gd_2O_3 particle size was about 1–2 nm according to the TEM data (Fig. 2*c*). The detailed characteristics of Gd_2O_3/GNFs was previously reported [16]. The graphitization (3rd step) and gas-phase modification (4th step) were earlier described [19, 20]. Graphitization (3rd step) prevented Gd_2O_3 degradation during the 4th step including surface oxidation of (Gd_2O_3/GNFs)@C particles.

The reaction of carboxyl groups in the (Gd_2O_3/GNFs)@C-COOH with $SOCl_2$ (5th step) is a well-known route of the carbon surface modification by acyl chloride groups [12–14]. This approach was previously described for surface modification of detonation nanodiamonds [21], single-walled carbon nanotubes [23], graphene oxide [24], etc. So, this reaction is suitable for modification of both sp^2- and sp^3-hybridized carbon atoms. The treatment of (Gd_2O_3/GNFs)@C-COOH particles with $SOCl_2$ did not affect the size and morphology of the GNFs or deposited Gd_2O_3 particles (Fig. 2*d-f*). The EELS confirmed the presence of C, O, Gd, and Cl atoms (Fig. 2*f*). The distribution of Gd atoms remained uniform (Fig. 2*e*, *f*).

Chloride groups could be substituted by other nucleophilic groups, such as SH in the captopril molecule or alloxide OAll fragment (6th step). The morphology of the (Gd_2O_3/GNFs)@C-COOAll (Fig. 2*g-i*) was similar to that of the pristine (Gd_2O_3/GNFs)@C-COCl particles (Fig. 2*d-f*).

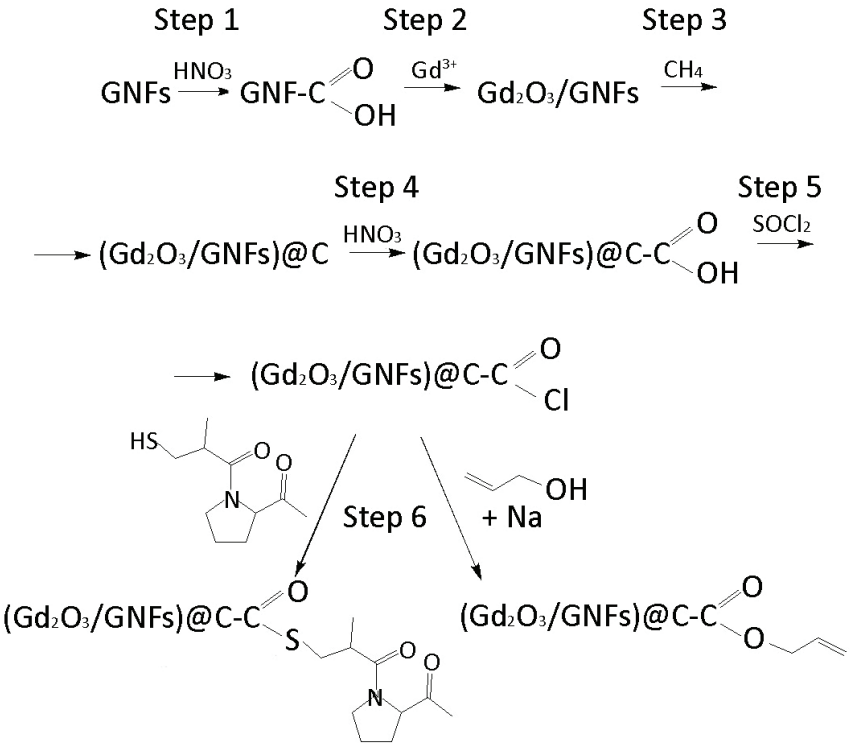

Fig. 1. Synthetic scheme

In $(Gd_2O_3/GNFs)$@C-captopril particles, some morphological changes occurred (Fig. 2*j*-*l*). GNFs partly bent (Fig. 2*j*) and lost their layered structure (Fig. 2*k*). At the same time, the in homogeneity of Gd-containing fragments became noticeable (Fig. 2*l*).

The chemical composition and bonding type of atoms in $(Gd_2O_3/GNFs)$@C-COOAll and $(Gd_2O_3/GNFs)$@C-captopril were confirmed by XPS. The XPS data for $(Gd_2O_3/GNFs)$@C-COOAll was discussed in [18]. The survey XPS spectra of $(Gd_2O_3/GNFs)$@C-captopril revealed the presence of O, C, N, Gd, Cl, and S (Fig. 3*a*). The XPS elemental composition of $(Gd_2O_3/GNFs)$@C-captopril was (at. %) C – 86.3, O – 11.0, N – 1.1, S – 0.6, Cl – 0.3, Gd – 0.4, and Si impurities – 0.3.

Fitting of the high-resolution C1s XPS spectrum of $(Gd_2O_3/GNFs)$@C-captopril revealed several components with binding energies of 284.5, 285.1, 286.3, 287.6, 288.8 eV corresponded to sp^2- and sp^3-hybridized C−C, C−O, ketone C=O, and carboxyl C(=O)−O species (Fig. 3*b*). The O1s spectrum shows three components at 531.5 eV (O=C), 533.3 eV (O–C), and 534.5 eV (non-conducting impurities) (Fig. 3*c*), which agrees with the different bonding of carbon atoms with oxygen observed in the C1s spectrum. The N1s spectrum contained components with binding energies of 398.6 eV (C−N=C), 400.1 eV (N−C=O), 402.0 eV (NR_4^+), and 405.8 eV (NO_2) (Fig. 3*d*). Oxidized nitrogen species were probably introduced to the surface during oxidation of carbon shells in the 4th step. The S2p spectra showed two doublets with $S2p_{3/2}$ binding energies of 163.6 eV (S–H and S–C) and 169.9 eV (SO_4^{2-} species) (Fig. 3*e*). The latter species resulted from the partial hydrolysis of sulfide groups. The gadolinium was in the Gd^{3+} state according to the Gd4d (Fig. 3*e*) and $Gd3d_{5/2}$ (Fig. 3*f*) spectra.

The IR transmittance spectra of $(Gd_2O_3/GNFs)$@C-COOH, $(Gd_2O_3/GNFs)$@C-COCl, $(Gd_2O_3/GNFs)$@C-COOAll, and $(Gd_2O_3/GNFs)$@C-captopril samples are shown in Fig. 4. The lines at 440–550 cm^{-1} are associated with Gd–O vibration in the Gd_2O_3 [25]. The IR spectra of GNFs, oxidized GNFs and $(Gd_2O_3/GNFs)$@C-COOH were discussed in [18, 26]. The lines of adsorbed water lay in the range of 3000–3700 cm^{-1}. These groups manifested in the $(Gd_2O_3/GNFs)$@C-COOH spectrum. The lines at 1640–1700 cm^{-1} correspond to the valent vibration of carbonyl or C=O fragment of carboxylic groups [26]. Lines typical to C–Cl and C–S vibrations in the $(Gd_2O_3/GNFs)$@C-COCl and $(Gd_2O_3/GNFs)$@C-captopril samples were not observed due to their low intensity. The IR spectra of captopril were previously described in [27]. Its characteristic lines were not observed in the $(Gd_2O_3/GNFs)$@C-captopril spectrum because of the low captopril content.

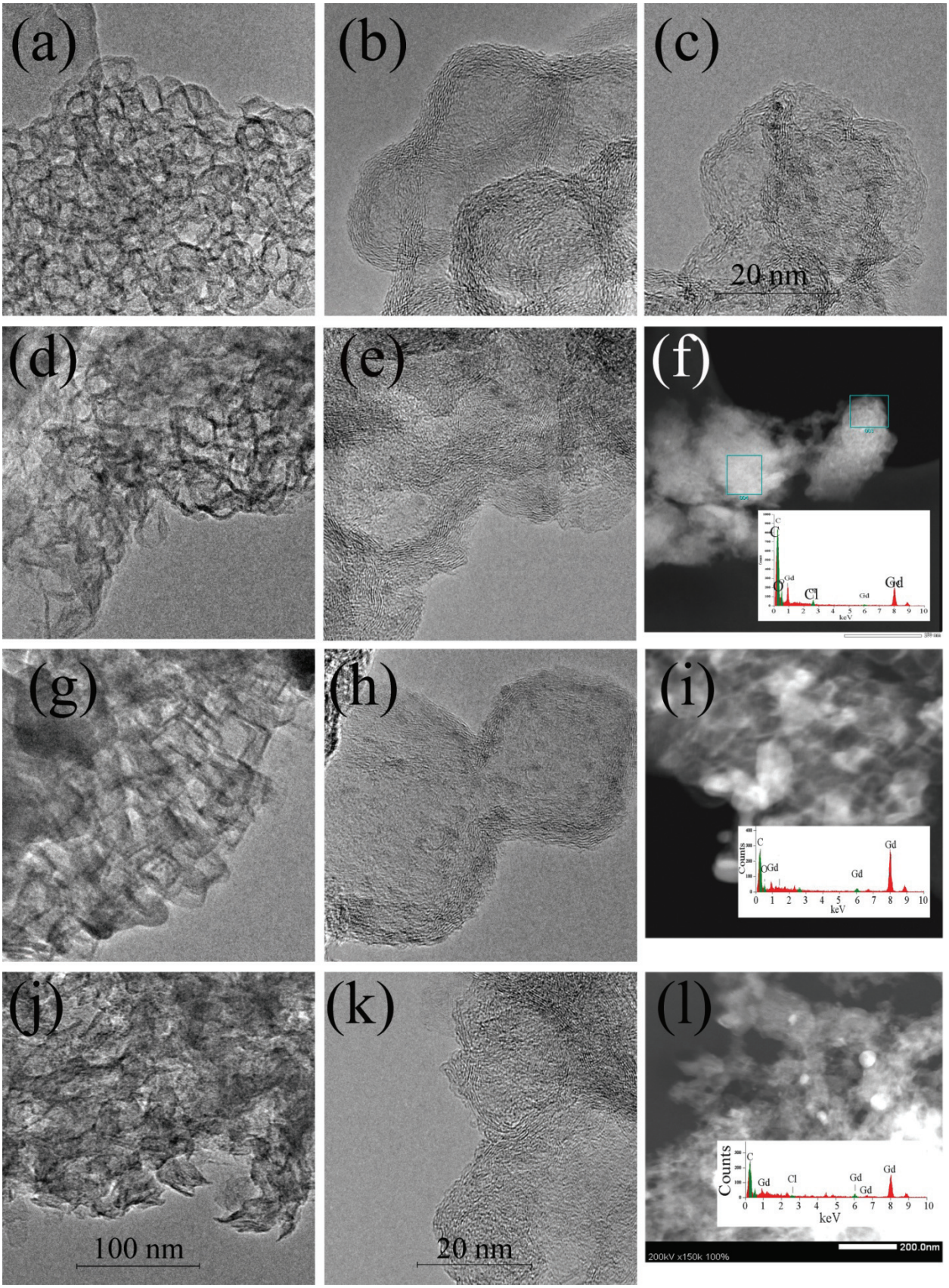

Fig. 2. TEM (*a*, *d*, *g*, *j*), HR TEM (*b*, *c*, *e*, *h*, *k*) and HAADF-STEM with EELS spectra (*f*, *i*, *l*) images of GNFs (*a*, *b*), Gd_2O_3/GNFs (*c*), (Gd_2O_3/GNFs)@C-COCl (*d* – *f*), (Gd_2O_3/GNFs)@C-COOAll (*g* – *i*) and (Gd_2O_3/GNFs)@C-captopril (*j* – *l*) particles. The scale of *a*, *d*, *g* images is the same as *j*. The scale of *b*, *e*, *h* images is the same as *k*

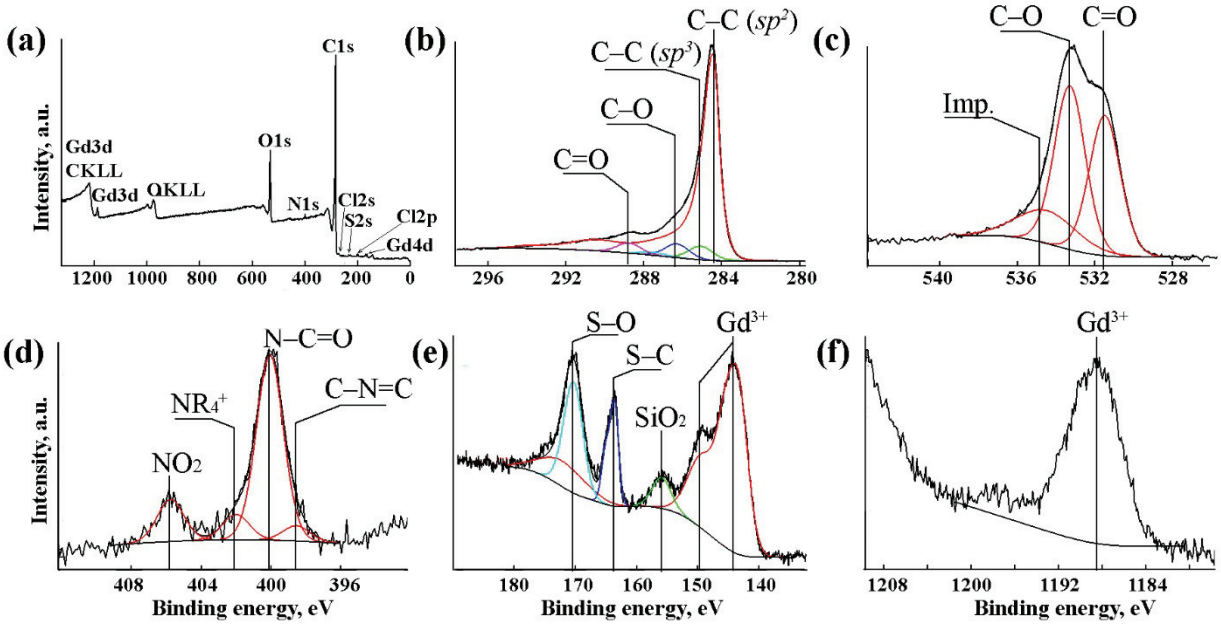

Fig. 3. Survey (*a*), and high resolution C1s (*b*), O1s (*c*), N1s (*d*), S2p, Si2s, Gd4d (*e*) and $Gd3d_{5/2}$ (*f*) XPS spectra of (Gd_2O_3/GNFs)@C-captopril sample

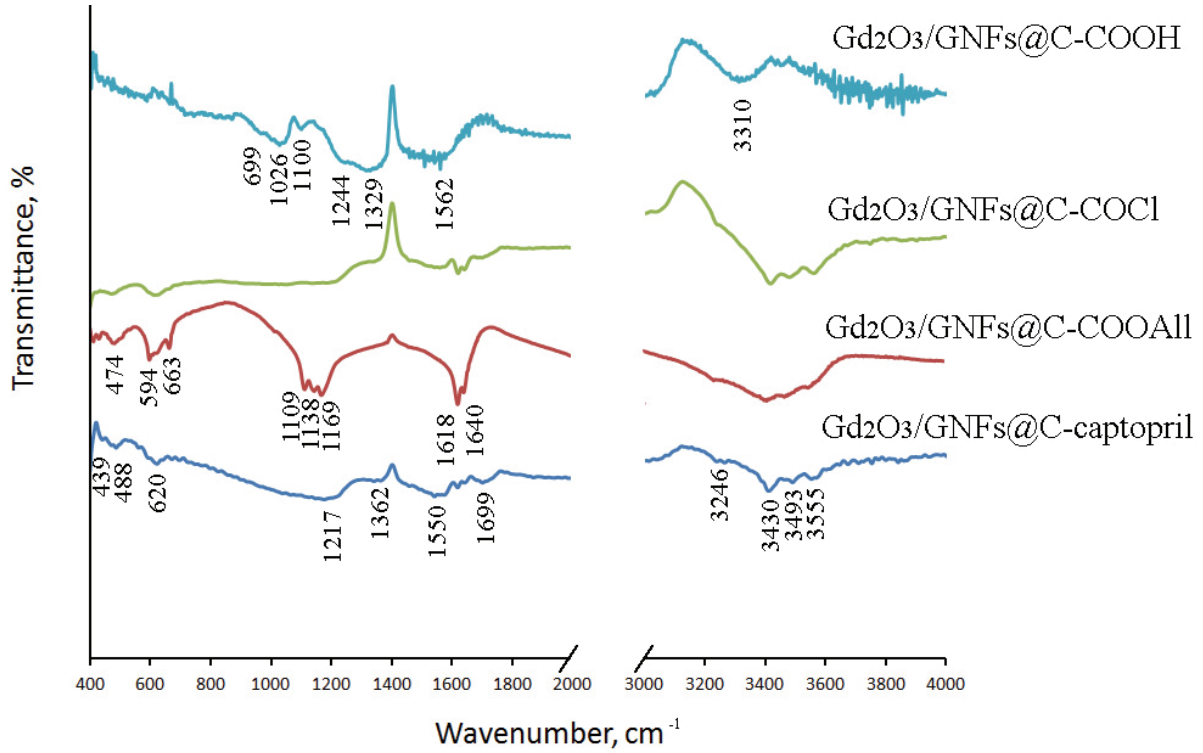

Fig. 4. IR transmittance spectra of (Gd_2O_3/GNFs)@C-COOH, (Gd_2O_3/GNFs)@C-COCl, (Gd_2O_3/GNFs)@C-COOAll, and (Gd_2O_3/GNFs)@C-captopril samples

TG and DTA of (Gd_2O_3/GNFs)@C-COCl (Fig. 5*a*), (Gd_2O_3/GNFs)@C-COOAll (Fig. 5*c*) and (Gd_2O_3/GNFs)@C-captopril (Fig. 5*d*) samples were performed under air atmosphere. Weight loss up to 200 °C is associated with the removal of adsorbed water and manifests itself as peaks on the DTG and DTA curves at 90 °C (maximum rate of weight loss) and 100 °C (endothermic effect), respectively. Next, the organic functional groups are removed and the GNFs burns, which is accompanied by the release of

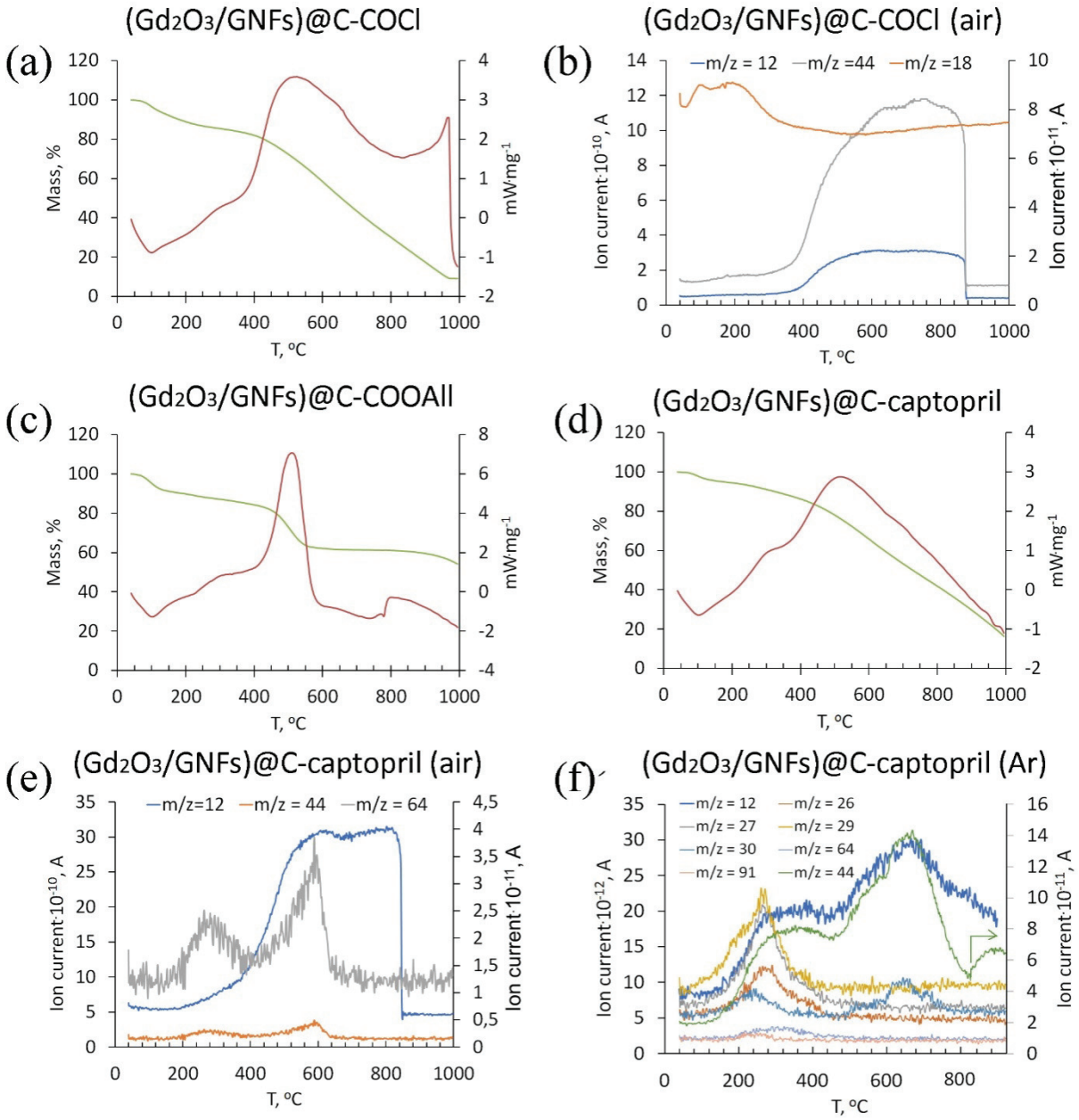

Fig. 5. TG (green) and DTA (red) curves (*a*, *c*, *d*) of (Gd_2O_3/GNFs)@C-COCl (*a*), (Gd_2O_3/GNFs)@C-COOAll (*c*) and (Gd_2O_3/GNFs)@C-captopril (*d*) samples. Gas products (*b*, *e*, *f*) of (Gd_2O_3/GNFs)@C-COCl under air atmosphere (*b*) and (Gd_2O_3/GNFs)@C-captopril under air (*e*) and Ar (*f*) atmospheres

heat. (Gd_2O_3/GNFs)@C-COCl burns completely to a residual mass of 9 %, due to Gd_2O_3 residue. According to the TG and DTG curves, (Gd_2O_3/GNFs)@C-COOAll and (Gd_2O_3/GNFs)@C-captopril don't burn completely, and their residual mass were 54 and 16 %, respectively. The data for (Gd_2O_3/GNFs)@C-captopril is close to the TG curves obtained for the composite Fe_3O_4@C_3N_4–Pr– captopril described in [15].

The defunctionalization was analyzed by mass-spectrometry of evolving gases (Fig. 5*b*, *e*, *f*). In air atmosphere, (Gd_2O_3/GNFs)@C-COCl sample decomposed in the range of 100–520 °C with releasing water ($m/z = 18$). The burn products corresponding to C ($m/z = 12$) and CO_2 ($m/z = 12$) appeared at 400–800 °C (Fig. 5*b*).

The GNF in (Gd_2O_3/GNFs)@C-captopril burnt under air atmosphere in the range of 400–600 °C with appearance of C ($m/z = 12$) and CO_2 ($m/z = 12$) signals in mass-spectra. The SO_2 ($m/z = 64$) signal was registered in the ranges of 200–400 °C and 450–600 °C. It can be associated with by-products of

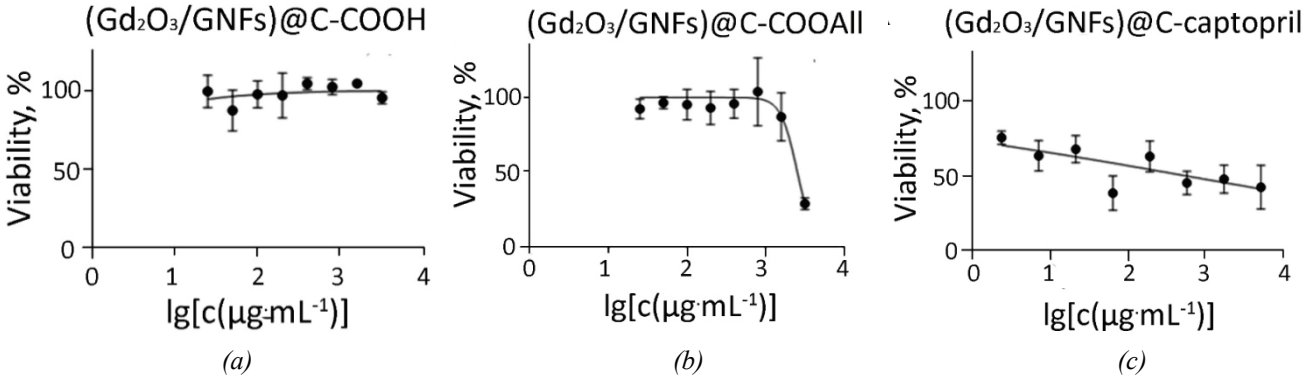

Fig. 6. The cytotoxicity of $(Gd_2O_3/GNFs)$@C-COOH (*a*), $(Gd_2O_3/GNFs)$@C-COOAll (*b*) and $(Gd_2O_3/GNFs)$@C-captopril (*c*) samples

the synthesis 5th step (Fig. 1) and burning of the captopril fragment (Fig. 5*e*).

In Ar atmosphere, the composition of gaseous products from $(Gd_2O_3/GNFs)$@C-captopril was more complex (Fig. 5*f*). C ($m/z = 12$) and CO_2 ($m/z = 44$) were observed at 200–420 °C and 550–700 °C as a result of defunctionalization and burning. The peaks with $m/z = 26$ ($C_2H_2^+$), 27 ($C_2H_3^+$), and 29 ($C_2H_5^+$) appeared at 180–380 °C in the mass spectra, while the peak with $m/z = 30$ (CH_2O^+) was observed in a wider range of temperatures. The by-product SO_2 ($m/z = 64$) was released at 250–400 °C. The peak with $m/z = 91$ corresponding to the captopril fragment appeared at 200–300 °C [28].

The results of cytotoxicity assessment for $(Gd_2O_3/GNFs)$@C-COOH, $(Gd_2O_3/GNFs)$@C-COOAll and $(Gd_2O_3/GNFs)$@C-captopril are presented in Fig. 6. For $(Gd_2O_3/GNFs)$@C-COOH (Fig. 6*a*), no substantial cytotoxicity signals were observed. $(Gd_2O_3/GNFs)$@C-COOAll showed a dose-specific cytotoxic effect on a cell line HEK293T (IC_{50abs} – (2555 ± 182) mg·L^{-1}) (Fig. 6*b*), that could be explained by presence of chemically active allyl groups on its surface. $(Gd_2O_3/GNFs)$@C-captopril (IC_{50abs} – (944 ± 58) mg·L^{-1}) triggered a dose-dependent decrease of cell viability over entire assessed range of concentrations (Fig. 6*c*). Such effect is uncommon for non-specific cytotoxicity and can potentially be explained by nanoparticle uptake by the cells during extended incubation [29]. According to *The Human Protein Atlas* data [30, 31], HEK293 cell lines express angiotensin-converting enzyme, creating a molecular target for binding of the synthesized nanoparticles functionalized by captopril. While this effect potentially increases the cytotoxicity of the contrast agent, it also increases its selectivity towards tissues with similar protein expression profile and allows their selective visualization. This effect requires further investigation to confirm its mechanism and assess its impact towards the pharmaco-toxicological profile of developed contrast agents considering their intended application for selective contrasting and at the same time the possibility of their local accumulation in high concentrations due to selective affinity.

4. Conclusion

The study presents a way to develop a fundamentally new type of multimodal contrast agents for MRI and computed tomography based on core-shell nanoparticles with insoluble core of a Gd^{3+} compound whose surface is modified with functional groups. A multistage synthesis of Gd_2O_3 nanoparticles stabilized with graphene matrix, coated with a graphite shell and surface-modified with carboxyl groups, acyl chloride, allyl fragments and, for the first time, captopril molecules was proposed. The size of Gd_2O_3 nanoparticles did not change during modification. Subsequent treatment with thionyl chloride resulted in acyl chloride formation on the particle surface, making it suitable for further specific functionalization. $(Gd_2O_3/GNFs)$@C particles covalently bound with captopril molecules were obtained for the first time. Considering the potential biomedical applications of the produced samples, their cytotoxicity was assessed. The observed cytotoxicity profile generally demonstrated the possibility of their use in biomedical imaging studies but confirmed the need for further extensive studies of their pharmaco-toxicological properties.

5. Funding

This research was supported by Russian Science Foundation No. 22-15-00072-П.

Финансирование

Исследование выполнено за счет средств гранта Российского научного фонда № 22-15-00072-П.

6. Acknowledgments

The authors acknowledge the support from the MSU Equipment Center "Nanochemistry and Nanomaterials", operating within the framework of the Lomonosov Moscow State University Program of Development.

Благодарности

Авторы выражают благодарность ЦКП МГУ «Нанохимия и наноматериалы», работающему в рамках Программы развития Московского государственного университета имени Ломоносова, за оказанную поддержку.

7. Conflict of interest

The authors declare no conflict of interest.

Конфликт интересов

Авторы заявляют об отсутствии конфликта интересов.

References

1. Najjar R. Clinical applications, safety profiles, and future developments of contrast agents in modern radiology: a comprehensive review. *iRadiology*. 2024;2(5):430-468. DOI:10.1002/ird3.95

2. Mhlanga N, Mphuthi N, Van der Walt H, Nyembe S, et al. Nanostructures and nanoparticles as medical diagnostic imaging contrast agents: a review. *Materials Today Chemistry*. 2024;40:102233. DOI:10.1016/j.mtchem.2024.102233

3. Meng YQ, Shi YN, Zhu YP, Liu YQ, et al. Recent trends in preparation and biomedical applications of iron oxide nanoparticles. *Journal of Nanobiotechnol*ogy. 2024;22:24. DOI:10.1186/s12951-023-02235-0

4. Lv J, Roy S, Xie M, Yang X, Guo B. Contrast agents of magnetic resonance imaging and future perspective. *Nanomaterials*. 2023;13(13):2003. DOI:10.3390/nano13132003

5. Abaei S, Tarighatnia A, Mesbahi A, Aghanejad A. Antibody conjugates as CT/MRI theranostics for diagnosis of cancers: a review of recent trends and advances. *Sensors Diagnostics*. 2024;3:1428-1441. DOI:10.1039/D4SD00132J

6. Kharisov BI, Dias HVR, Kharissova OV, Vázquez A, et al. Solubilization, dispersion and stabilization of magnetic nanoparticles in water and non-aqueous solvents: recent trends. *RSC Advances*. 2014;4:45354-45381. DOI:10.1039/C4RA06902A

7. Suslova EV, Pavlova OS, Zoirova ZO, Shashurin DA, et al. Gd_2O_3@C and Gd_2O_3@SiO_2 nanoparticles as contrast agents for magnetic resonance imaging. *Zhurnal prikladnoy khimii = Russian Journal of Applied Chemistry*. 2025;98(2):125-135. DOI:10.31857/S0044461825020055 (In Russ.)

8. Ahren M, Selegard L, Klasson A, Soderlind F, et al. Synthesis and characterization of PEGylated Gd_2O_3 nanoparticles for MRI contrast enhancement. *Langmuir*. 2010;26(8):5753-5762. DOI:10.1021/la903566y

9. Fatima A, Ahmad MW, Al Saidi AKA, Choudhury A, et al. Recent advances in gadolinium based contrast agents for bioimaging applications. *Nanomaterials*. 2021;11(9):2449. DOI:10.3390/nano11092449

10. Pour SA, Shaterian HR. Captopril-loaded superparamagnetic nanoparticles as a new dual-mode contrast agent for simultaneous in vitro/in vivo MR imaging and drug delivery system. *Pharmaceutical Chemistry Journal*. 2018;51(10):852-862. DOI:10.1007/s11094-018-1704-x

11. Lam E, Luong HT. Carbon materials as catalyst supports and catalysts in the transformation of biomass to fuels and chemicals. *ACS Catalysis*. 2014;4(10):3393-3410. DOI:10.1021/cs5008393

12. Kulakova LI, Lisichkin GV. Chemical modification of graphene. *Russian Journal of General Chemistry*. 2020;90(10):1921-1943. DOI:10.1134/S1070363220100151

13. Joshi DJ, Koduru JR, Malek NI, Hussain CM, Kailasa SK. Surface modifications and analytical applications of graphene oxide: a review. *TrAC Trends in Analytical Chemistry*. 2021;144:116448. DOI:10.1016/j.trac.2021.116448

14. Yu W, Sisi L, Haiyan Y, Jie L. Progress in the functional modification of graphene/graphene oxide: a review. *RSC Advances*. 2020;10(26):15328-15345. DOI:10.1039/d0ra01068e

15. Rezaei F, Alinezhad H, Maleki B. Captopril supported on magnetic graphene nitride, a sustainable and green catalyst for one-pot multicomponent synthesis of 2-amino-4*H*-chromene and 1,2,3,6-tetrahydropyrimidine. *Scientific Reports*. 2023;13:20562. DOI:10.1038/s41598-023-47794-2

16. Suslova EV, Kozlov AP, Shashurin DA, Rozhkov VA, et al. New composite contrast agents based on Ln and graphene matrix for multi-energy computed tomography. *Nanomaterial*s. 2022;12:4110. DOI:10.3390/nano12234110

17. Shashurin DA, Suslova EV, Rozhkov VA, Sotenskiy RV, et al. Gd_2O_3-carbon nanoflakes (CNFs) as contrast agents for photon-counting computed tomography (PCCT). *Zhurnal prikladnoy khimii = Russian Journal of Applied Chemistry*. 2023;96(4):337-344. DOI:10.31857/S0044461823040023 (In Russ.)

18. Suslova EV, Shashurin DA, Maslakov KI, Kupreenko SY, et al. Composite contrast enhancement of

hydrogel-based implants for photon-counting computed tomography studies. *Gels*. 2024;10(12):807. DOI:10.3390/gels10120807

19. Kozlov AP, Suslova EV, Maksimov SV, Isaikina OY, et al. The preparation of nanocomposite with a core-shell structure made of carbon matrices and lanthanum nanoparticles. *Physics of Particles and Nuclei Letters.* 2023;20:1254-1258. DOI:10.1134/S1547477123050473

20. Suslova EV, Kozlov AP, Shashurin DA, Maximov SV, et al. La_2O_3-carbon composite with core-shell structure and features of its gas-phase oxidation. *Mendeleev Communications*. 2024;34(1),90-92. DOI:10.1016/j.mencom.2024.01.027

21. Sivtsov EV, Kalinin AV, Gostev AI, Smirnov AV, et al. In situ preparation of polymer nanocomposites based on sols of surface-modified detonation nanodiamonds by classical and controlled radical polymerization. *Polymer Science Series B*. 2020;62:734-749. DOI:10.1134/S1560090420050139

22. Chesnokov VV, Chichkan AS, Bedilo AF, Shuvarakova EI, Parmon VN. Template method for graphene synthesis. *Doklady Akademii Nauk = Doklady Chemistry*. 2019;488:508-512. DOI:10.31857/S0869-56524885508-512 (In Russ.)

23. Hamon MA, Chen J, Hu H, Chen Y, et al. Dissolution of single-walled carbon nanotubes. *Advanced Materials*. 1999;11(10):834-840.

24. Yao J, Liu S, Huang Y, Ren S, et al. Acyl-chloride functionalized graphene oxide chemically grafted with hindered phenol and its application in anti-degradation of polypropylene. *Progress in Natural Science: Materials International*. 2020;30(3):328-336. DOI:10.1016/j.pnsc.2020.05.010

25. Vijayaprasath G, Habibulla I, Dharuman V, Balasubramanian S, Ganesan R. Fabrication of Gd_2O_3 nanosheet-modified glassy carbon electrode for nonenzymatic highly selective electrochemical detection of vitamin B2. *ACS Omega*. 2020;5(29):17892-17899. DOI:10.1021/acsomega.9b04284

26. Brusko V, Khannanov A, Rakhmatullin A, Dimiev AM. Unraveling the infrared spectrum of graphene oxide. *Carbon*. 2024;229:119507. DOI:10.1016/j.carbon.2024.119507

27. Chepilo DA, Gegechkori VI, Shchepochkina OYu, Efremov AYu, et al. A complex approach to the determination of authenticity in the development of standard samples for ace inhibitors. *Khimiko-farmatsevticheskiy zhurnal = Pharmaceutical Chemistry Journal*. 2022;56(4):515-521. DOI:10.30906/0023-1134-2022-56-4-41-47 (In Russ.)

28. Chepilo DA, Gegechkori VI, Shchepochkina OYu, Chadova NN, et al. Application of the gas chromatography-mass spectrometry method for the identification of standard samples of ACE inhibitors drugs. *Farmatsiya*. 2022;71(3):34-41. DOI:10/29296/25419218-2022-03-06 (In Russ.)

29. Verkhovsky RA, Anisimov RA, Lomova MV, Tuchina DK, et al. Cytotoxicity of various types of coated upconversion nanoparticles. Overview. *Izvestiya of Saratov University. Physics*. 2022;22(4):357-373. DOI:10.18500/1817-3020-2022-22-4-357-373 (In Russ.)

30. Uhlén M, Fagerberg L, Hallström BM, Lindskog C, et al. Tissue-based map of the human proteome. *Science*. 2015;347(6220):1260419. DOI:10.1126/science.1260419

31. Jin H, Zhang C, Zwahlen M, von Feilitzen K, et al. Systematic transcriptional analysis of human cell lines for gene expression landscape and tumor representation. *Nature Communications.* 2023;14(1):5417. DOI:10.1038/s41467-023-41132-w

Information about the authors / Информация об авторах

Evgeniya V. Suslova, Cand. Sc. (Chem.), Senior Researcher, Chemistry Department, Lomonosov Moscow State University (MSU), Moscow, Russian Federation; ORCID 0000-0003-1945-9842; e-mail: suslova@kge.msu.ru

Суслова Евгения Викторовна, кандидат химических наук, старший научный сотрудник, Московский государственный университет имени М. В. Ломоносова (МГУ), Москва, Российская Федерация; ORCID 0000-0003-1945-9842; e-mail: suslova@kge.msu.ru

Sergey V. Yakovlev, Engineer, Kurnakov Institute of General and Inorganic Chemistry RAS (IGIC RAS), Moscow, Russian Federation; ORCID 0009-0004-1717-950X; e-mail: admin@viam.ru

Яковлев Сергей Викторович, инженер, Институт общей и неорганической химии им. Н. С. Курнакова РАН (ИОНХ РАН), Москва, Российская Федерация; ORCID 0009-0004-1717-950X; e-mail: admin@viam.ru

Denis A. Shashurin, Cand. Sc. (Med.), Senior Researcher, Medicine Research-Educational Institute, MSU, Moscow, Russian Federation; E.I. Chazov National Medical Research Center of Cardiology, Moscow, Russian Federation; ORCID 0000-0003-3463-5963; e-mail: shashurin@mail.ru

Шашурин Денис Александрович, кандидат медицинских наук, старший научный сотрудник, Медицинский научно-образовательный институт, МГУ, Москва, Российская Федерация; Национальный медицинский исследовательский центр кардиологии имени академика Е. И. Чазова, Москва, Российская Федерация; ORCID 0000-0003-3463-5963; e-mail: shashurin@mail.ru

Daria A. Ipatova, PhD Student, Chemistry Department, MSU, Moscow, Russian Federation; e-mail: ipatova.daria@yandex.ru

Dmitry A. Skvortsov, Cand. Sc. (Chem.), Associate Professor, Chemistry Department, MSU, Moscow, Russian Federation; ORCID 0000-0001-8336-8596; e-mail: skvorratd@mail.ru

Sergey V. Maximov, Engineer, Chemistry Department, MSU, Moscow, Russian Federation; e-mail: irber@yandex.ru

Konstantin I. Maslakov, Cand Sc. (Phys. and Math.), Senior Researcher, Chemistry Department, MSU, Moscow, Russian Federation; ORCID 0000-0002-0672-2683; e-mail: nonvitas@gmail.com

Yana B. Platonova, Cand Sc. (Chem.), Researcher, Chemistry Department, MSU, Moscow, Russian Federation; ORCID 0000-0001-6846-3421; e-mail: knoposk@inbox.ru

Serguei V. Savilov, D. Sc. (Chem.), Leading Researcher, Chemistry Department, MSU, Moscow, Russian Federation; IGIC RAS, Moscow, Russian Federation; ORCID 0000-0002-5827-3912; e-mail: savilov@chem.msu.ru

Georgy A. Chelkov, Cand Sc. (Phys. and Math.), Leading Researcher, Chemistry Department, MSU, Moscow, Russian Federation; Joint Institute for Nuclear Research, Dubna, Russian Federation; ORCID 0000-0002-3468-9761; e-mail: chelkov@jinr.ru

Ипатова Дарья Андреевна, аспирант, Химический факультет, МГУ, Москва, Российская Федерация; e-mail: ipatova.daria@yandex.ru

Скворцов Дмитрий Александрович, кандидат химических наук, доцент, Химический факультет, МГУ, Москва, Российская Федерация; ORCID 0000-0001-8336-8596; e-mail: skvorratd@mail.ru

Максимов Сергей Владимирович, инженер, Химический факультет, МГУ, Москва, Российская Федерация; e-mail: irber@yandex.ru

Маслаков Константин Игоревич, кандидат физико-математических наук, старший научный сотрудник, Химический факультет, МГУ, Москва, Российская Федерация; ORCID 0000-0002-0672-2683; e-mail: nonvitas@gmail.com

Платонова Яна Борисовна, кандидат химических наук, научный сотрудник, Химический факультет, МГУ, Москва, Российская Федерация; ORCID 0000-0001-6846-3421; e-mail: knoposk@inbox.ru

Савилов Сергей Вячеславович, доктор химических наук, заведующий лабораторией, ведущий научный сотрудник, Химический факультет, МГУ, Москва, Российская Федерация; ИОНХ РАН, Москва, Российская Федерация; ORCID 0000-0002-5827-3912; e-mail: savilov@chem.msu.ru

Шелков Георгий Александрович, кандидат физико-математических наук, ведущий научный сотрудник, заведующий лабораторией, Химический факультет, МГУ, Москва, Российская Федерация; Международная межправительственная организация «Объединенный институт ядерных исследований», Дубна, Российская Федерация; ORCID 0000-0002-3468-9761; e-mail: chelkov@jinr.ru

Received 09 October 2025; Revised 28 November 2025; Accepted 02 December 2025